

Sulfur Atoms as Tethers for Selective Attachment of Aromatic Molecules to Silicon(001) Surfaces

Sarah K. Coulter,* Michael P. Schwartz, and Robert J. Hamers

Department of Chemistry, University of Wisconsin—Madison, 1101 University Avenue, Madison, Wisconsin 53706

Received: October 31, 2000; In Final Form: January 29, 2001

Benzenethiol ($\text{C}_6\text{H}_5\text{SH}$) and diphenyl disulfide ($\text{C}_6\text{H}_5\text{S}-\text{SC}_6\text{H}_5$) were used as model systems to compare the interaction of chemically similar π -conjugated molecules with the Si(001)- 2×1 surface. The bonding behavior of these substituted aromatic hydrocarbons on the Si(001) surface was investigated using Fourier transform infrared spectroscopy (FTIR), X-ray photoelectron spectroscopy (XPS), and scanning tunneling microscopy (STM). Both FTIR and XPS indicate that benzenethiol molecules chemisorb on the Si(001) surface predominantly through the sulfur atom via deprotonation of the thiol substituent group. There also is evidence that a small minority of benzenethiol molecules may adsorb on the surface through the phenyl ring or undergo further fragmentation. Diphenyl disulfide appears to bond to the Si(001) surface in one primary configuration in which the S–S bond of diphenyl disulfide is cleaved and the two sulfur–phenyl moieties are bonded to the silicon surface through the sulfur atoms. Thermal studies indicate that the sulfur-tethered aromatic rings of benzenethiol and diphenyl disulfide are stable to temperatures above 520 K. Furthermore, STM studies show that these molecules chemisorb to the silicon surface within a single dimer row and, in the case of diphenyl disulfide, appear to form ordered rows of sulfur-tethered aromatic rings. This new chemistry demonstrates remarkable potential as a means of selectively attaching π -conjugated systems to technologically useful semiconductor surfaces.

Introduction

The Si(001) surface is the starting material for most microelectronic devices.¹ Although present microelectronic manufacturing techniques utilize inorganic precursors, there has been increased interest in employing organic materials for a variety of microelectronic and molecular electronic applications, including organic-based transistors, light-emitting diodes, and chemical/biological sensors.^{2,3} While the physical properties of individual molecules often can be measured and predicted, to be technologically useful it is necessary to be able to understand and control how these properties are affected by bonding to the surface. Accordingly, there is great interest in developing new methods for selectively attaching molecules to surfaces in such a way that the desired physical and chemical characteristics of the molecule are preserved.

For applications in molecular electronics, the electrical conductivity of molecules and molecular layers is of paramount importance. Electrical conductivity in organic molecules is typically associated with conjugated π -electron systems that permit delocalization of the electrons. Aromatic rings are often incorporated into these molecules because the rigidity and multiplicity of electron paths facilitate electron transport.⁴ Consequently, molecules with conjugated π -electron systems have electrical characteristics such that they can be considered to behave like “molecular wires”.^{5–11} Several recent studies have focused on measuring the electrical conductivity of π -conjugated molecules tethered to gold surfaces through external sulfur atoms^{10,11} and even have shown that such molecules can be used

as resonant-tunneling transistors.¹² Electrical conductivity via indirect interactions between aromatic rings, or “ π -stacking”, also has been implicated as playing an important role in electron transport in biological molecules, such as DNA.^{13–15} Transport via this indirect process is generally less favorable than that in directly conjugated systems, as evidenced by the anisotropic conductivity in graphite.¹⁶ Because of these interesting electrical properties, the behavior of benzene and related aromatic systems is of fundamental importance in the field of molecular electronics and has relevance in fields as diverse as the biological sciences and polymer chemistry.

For π -conjugated molecules to be used as conductors or semiconductors, they must retain π -conjugation, even after adsorption. Benzene, a simple π -conjugated ring, is known to chemisorb on the Si(001) surface by forming Si–C bonds.^{17–24} However, the formation of these new Si–C bonds results in the loss of π -conjugation and therefore is expected to dramatically decrease the electron transport capabilities of the molecule. The remaining π -electrons of the chemisorbed benzene are no longer delocalized over the entire molecule but, instead, remain in isolated double bonds.

Because the electronic properties of molecules such as benzene often are compromised upon chemisorption, there is interest in developing chemical attachment strategies that involve well-defined molecule–surface interfaces that preserve the desired electronic characteristics of the free molecule.³ One approach is to utilize specific functional groups that are not an intrinsic part of the delocalized π -system but which can tether the molecule of interest to the surface. For example, styrene ($\text{C}_6\text{H}_5\text{CH}=\text{CH}_2$) is known to selectively bond to the Si(001) surface through the external vinyl substituent group.²⁵ Because

* To whom correspondence should be addressed. Phone: (608) 262-9081. Fax: (608) 262-0453. E-mail: coulter@chem.wisc.edu.

the C=C bond external to the ring exclusively interacts with the surface, the π -conjugation of the aromatic ring remains unperturbed upon chemisorption.

Previous studies have used external substituent groups to successfully link π -conjugated molecules to gold.^{5–9,26–28} In particular, sulfur-containing functional groups, such as thiol, sulfide, or disulfide end groups, have been widely used to selectively tether large multifunctional organic molecules to gold surfaces.^{29–31} In some cases, these sulfur-terminated molecules will pack into well-ordered and well-oriented organic monolayers.^{32,33} One of the reasons these self-assembled monolayers pack so well is that the Au–S bond is weak, allowing for diffusion of the molecules on the surface. However, as a result of the weakly covalent Au–S bond (30–35 kcal/mol for aliphatic adsorbates), the monolayer is susceptible to degradation by heat or exposure to ozone.^{29,34,35}

Stronger covalent bonds between sulfur groups and a surface could increase the robustness of the monolayer. Selective adsorption of sulfur-containing molecules to the Si(001) surface results in strong covalent S–Si bonds (~ 54 kcal/mol),³⁶ producing more stable organic films. Furthermore, the inherent order of the Si(001) surface could serve as a template for preparing tethered arrays of organic molecules on the surface with greatly enhanced chemical and structural homogeneity. In this paper we explore a chemistry for linking π -conjugated molecules to the Si(001) surface using thiol (SH) and disulfide (SS) functional groups.

Experimental Section

Three different techniques were used to characterize the interaction of benzenethiol ($\text{C}_6\text{H}_5\text{SH}$) and diphenyl disulfide ($\text{C}_6\text{H}_5\text{S}-\text{SC}_6\text{H}_5$) with the Si(001) surface. The chemical composition and oxidation states of the adsorbed species were examined using X-ray photoelectron spectroscopy (XPS). Multiple internal reflection Fourier transform infrared (MIR-FTIR) spectroscopy was used to probe the vibrational modes of benzenethiol and diphenyl disulfide adsorbed on the Si(001) surface. The spatial distributions of the adsorbed molecules on the Si(001) surface were imaged using a home-built scanning tunneling microscope. All experiments were performed in ultra-high-vacuum (UHV) chambers with base pressures of $<3 \times 10^{-10}$ Torr.

Silicon(001) Samples. Silicon is tetrahedrally coordinated. The Si(001) surface undergoes a surface reconstruction in which the two dangling bonds of one silicon atom interact with the two dangling bonds of an adjacent silicon atom to produce a single silicon dimer ($\text{Si}=\text{Si}$). This interaction results in a (2×1) -reconstructed surface of highly ordered rows of silicon dimers.^{37,38}

The studies presented in this paper were performed using Si(001) wafers oriented to the (001) surface within $\pm 0.5^\circ$ (Wacker Chemitronics). Silicon samples used in XPS and scanning tunneling microscopy (STM) experiments were cut from polished n-type, Sb-doped, low-resistivity wafers (0.010 – $0.020 \Omega \text{ cm}$). Lightly doped wafers were used in MIR-FTIR studies to minimize free-carrier absorption. The MIR-FTIR silicon samples were cut from p-type, B-doped wafers ($15 \Omega \text{ cm}$) that were polished on both large ($0.9 \text{ cm} \times 2.0 \text{ cm}$) faces. The two small edges ($0.9 \text{ cm} \times 0.7 \text{ mm}$) of the samples were polished at 45° off the (001) face to create a trapezoidal prism for use in a multiple internal reflection geometry.^{39,40} All samples were rinsed in electronic grade methanol and cleaned of residual surface carbon contamination by exposure to ozone for 15 min. After being transferred to a vacuum, the samples were outgassed overnight at 850 K and then annealed at 1400 K to remove the oxide layer. This procedure has been shown

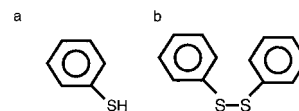


Figure 1. Structure of (a) benzenethiol and (b) diphenyl disulfide.

to produce a clean, well-ordered (2×1) -reconstructed Si(001) surface.⁴¹

Techniques. XPS measurements were performed using a Physical Electronics system with a monochromatized Al K α source and a hemispherical analyzer with a 16-channel detector array. The silicon(2p) and carbon(1s) regions were probed with a pass energy of 5.85 eV. A broad, intense peak, due to emission from a silicon plasmon, interferes with the sulfur(2p) signal. Therefore, the lower-intensity sulfur(2s) region was measured. To increase signal intensity, the hemispherical analyzer pass energy was increased to 23.5 eV when the sulfur(2s) region was scanned. After a Shirley background correction was performed,⁴² the XPS data were fit to Voight (Gaussian–Lorentzian convolution) peak shapes using a commercial software package (Wavemetrics). The quality of fit was evaluated using a reduced χ^2 .⁴³ Reduced χ^2 values of 1.0 or less indicate that the fit is statistically equivalent to the observed spectrum.

The Si(2p) region was measured in each XPS study and used as an internal standard for both binding energies and integrated peak intensities. The two Si(2p) peaks were corrected to the bulk binding energies of 99.4 and 100.0 eV corresponding to the $\text{Si}(2p)_{3/2}$ and $\text{Si}(2p)_{1/2}$ lines, respectively. The same correction, typically less than 0.6 eV, was applied to the binding energies of the C(1s) and S(2s) peaks. This correction ensures that the core-level shifts reported here are due solely to changes in the local chemical environment and not changes due to band-bending effects resulting from adsorption.

For MIR-FTIR studies, infrared light from a Mattson RS-1 FTIR spectrometer was coupled into the narrow edge of a clean, polished silicon sample. Infrared light entered and exited the UHV chamber via BaF_2 windows and, after exiting the chamber, was collected with a cooled InSb detector.⁴⁰ All MIR-FTIR spectra were acquired with 4 cm^{-1} resolution. Spectra of liquid benzenethiol and solid diphenyl disulfide were obtained under ambient conditions using a Nicolet 740 FTIR with a triglycine sulfate (TGS) detector at 1 cm^{-1} resolution.

STM was used to image benzenethiol and diphenyl disulfide on the Si(001) surface at submonolayer coverages. Images were obtained with a tunneling current of 100 pA. Although images were acquired with sample biases ranging from -1.5 to -4.5 V, the best images were obtained at sample biases between -2.2 and -2.8 V.

Molecules Studied. Benzenethiol ($\text{C}_6\text{H}_5\text{SH}$, 99+%), diphenyl disulfide ($\text{C}_6\text{H}_5\text{S}-\text{SC}_6\text{H}_5$, 99%), and styrene ($\text{C}_6\text{H}_5\text{CH}=\text{CH}_2$, 99%) were purchased from Aldrich; each compound was further purified by at least three freeze–pump–thaw cycles. The structures of benzenethiol and diphenyl disulfide are presented in Figure 1.

Isotopic studies were conducted to distinguish between decomposition by S–H and C–H bond cleavage. Deuterated benzenethiol ($\text{C}_6\text{H}_5\text{SD}$) was prepared by shaking equal volumes of benzenethiol (99+%, Aldrich) and deuterium oxide (99.9%, CDN) for 4–6 h.^{44,45} The benzenethiol was decanted, and a new aliquot of deuterium oxide was added. This procedure was repeated two more times with the same benzenethiol sample. After decanting for the third time, a small amount of anhydrous magnesium sulfate was added to absorb any remaining deuterium oxide. The solution was decanted and then fractionally distilled under a reduced pressure of approximately 30 Torr.

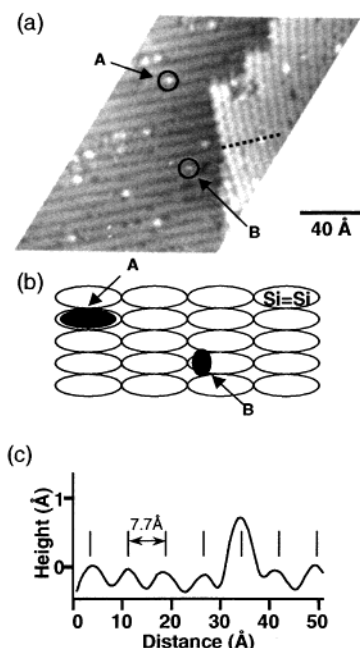


Figure 2. (a) STM image of a clean Si(001) surface exposed to 0.18 L (5.0×10^{-9} Torr for 35 s) of benzenethiol. Image acquired at -2.20 V. Surface adsorbates appear as bright protrusions. Counting statistics indicate feature A accounts for approximately 95% of surface features. (b) Schematic drawing showing the positions of feature A and feature B adsorbates relative to the silicon dimers. Solid black ovals represent surface adsorbates, while empty ovals represent the silicon dimers. (c) Line profile over feature A as indicated by the dashed line in Figure 3a. Vertical hashes represent spacing between dimer rows (7.7 Å).

The benzenethiol-SD fraction had a boiling point of 72 °C at 30 Torr. ^1H NMR spectra of the benzenethiol-SD sample showed a series of ring peaks between 7.315 and 6.898 ppm and a small S–H peak intensity at 3.423 ppm. By comparing the integrated areas of the ring peaks and the S–H peak, we concluded that the benzenethiol-SD is approximately 92% deuterated. ^2H NMR spectra showed that the hydrogen–deuterium substitution occurs only on the thiol substituent group, leaving the ring completely unaltered.

Some thiols are known to decompose via a reaction with stainless steel.^{28,46} To minimize unwanted decomposition, the gas lines of the UHV chambers were baked overnight and passivated by cycles of filling and purging prior to each dosing. The chemicals were introduced to the UHV chambers through a variable leak valve with an attached tube directed toward the surface. Overall purity was verified with an in situ mass spectrometer. In the case of benzenethiol-SD, however, the possibility of isotopic H–D exchange on the walls of the chamber cannot be ruled out. Exposures were estimated from chamber pressure and time of exposure (1 L = 1 langmuir = 1.0×10^{-6} Torr for 1 s). Actual exposure at the surface was likely higher due to the geometry of the chambers.

Results

Benzenethiol. Figure 2a is an STM image of a Si(001) surface exposed to 0.18 L of benzenethiol at 300 K, imaged at a sample bias of -2.20 V. Two kinds of absorption features are observed. Both features appear as bright protrusions but differ in their symmetry with respect to the underlying dimers, as indicated in Figure 2b. The primary species, A, is centered within a single dimer row, covering 1 – 2 dimers. The secondary feature, B, is a smaller, bright feature, off-center with respect to a single dimer within a row. Counting statistics indicate that feature A accounts

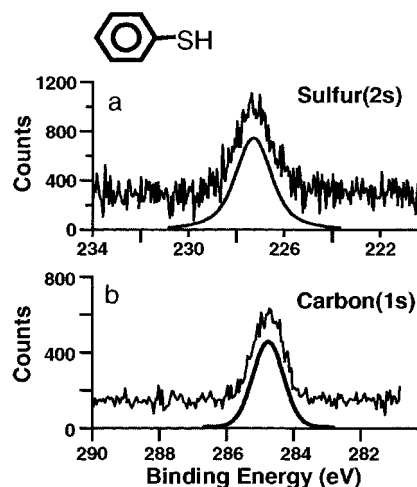


Figure 3. XPS data of a clean Si(001) surface exposed to 5.0 L (2.5×10^{-8} Torr for 200 s) of benzenethiol for the (a) S(2s) and (b) C(1s) regions. Solid lines below represent the fitted peak.

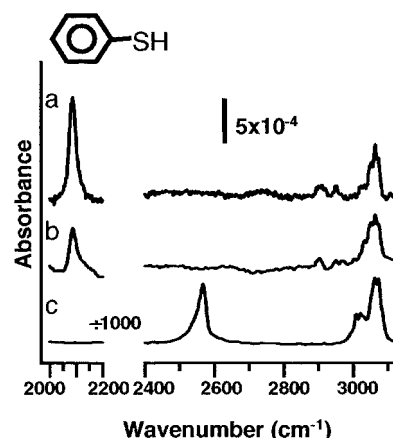


Figure 4. FTIR spectra of benzenethiol: (a) a clean Si(001) surface at 300 K exposed to 3.0 L (3.0×10^{-8} Torr for 100 s) of benzenethiol, (b) a clean Si(001) surface at 300 K exposed to 3.0 L (1.0×10^{-8} Torr for 300 s) of benzenethiol-SD; (c) liquid benzenethiol.

for $>95\%$ of the total features observed; feature B is a minor secondary product that could be associated with defects on the Si(001) substrate. These images indicated that the vast majority of molecules bond into one configuration.

Figure 2c is a line profile over feature A, as indicated by the dashed line in the STM image. From this line profile, it is apparent that feature A is almost centered with respect to a single dimer row, protruding an average height of 0.7 Å from the top of the surface dimers.

To identify the changes in bonding accompanying adsorption, XPS spectra were obtained of a Si(001) surface exposed to 5.0 L of benzenethiol at 300 K, as shown in Figure 3. The spectra for both the S(2s) region and the C(1s) region were each fitted with a single Voight curve, represented by the solid lines in Figures 3a and 3b, respectively. The S(2s) region in Figure 3a can be fit to a single peak with an energy of 227.3 eV (fwhm = 0.94 eV) and a reduced χ^2 value of 0.9 . Similarly, the C(1s) region in Figure 3b can be fit to a single peak with an energy of 284.8 eV (fwhm = 1.04 eV, $\chi^2 = 1.0$).

The FTIR spectra of benzenethiol are presented in Figure 4. Figure 4a shows the FTIR spectrum of a Si(001) surface exposed to 3.0 L of benzenethiol at 300 K. Higher exposures of benzenethiol yielded no changes in the spectrum. This absence of change indicates that a 3 L exposure of benzenethiol results in a fully saturated, self-terminating monolayer. Absorption

TABLE 1: Modes and Associated Frequencies of Benzenethiol⁴⁷ and Benzenethiol/Si(001)

mode	benzenethiol (cm ⁻¹)	benzenethiol adsorbed on Si(001) (cm ⁻¹)
13	3037	3023
7b	3048	3050
2	3056	3064
20a	3086	3073
ν SH	2575	none

features are present in three distinct regions. Peaks between 3000 and 3100 cm⁻¹ commonly correspond to absorbances of aromatic or sp²-hybridized C–H stretches. Four distinct peaks are located in this region at 3023, 3049, 3063, and 3074 cm⁻¹. Two smaller peaks, at 2908 and 2952 cm⁻¹, are located in the region typically associated with sp³-hybridized C–H stretches. A single, large peak at 2086 cm⁻¹ is present in the region corresponding to silicon–hydrogen stretching modes.

The observation of a peak associated with silicon–hydrogen vibrations indicates that adsorption is accompanied by cleavage of S–H and/or C–H bonds. To distinguish between these possibilities, experiments were performed using C₆H₅SD. The FTIR spectrum of a Si(001) sample exposed to 3.0 L of C₆H₅SD is presented in Figure 4b. To compare the changes in the silicon–hydrogen peaks, it is necessary to account for changes in the intensity of the two spectra due to differences in alignment between samples. Because the intensities of the peaks due to C–H ring stretching modes should be the same for a C₆H₅SH sample and a C₆H₅SD sample, spectra were normalized to the area of the C–H peaks in the region between 2800 and 3100 cm⁻¹. The normalized area ratio $A_{\text{SiH}}/A_{\text{CH}}$ in Figure 4a is 0.0268. In comparison, the $A_{\text{SiH}}/A_{\text{CH}}$ in Figure 4b is 0.0087. Thus, exposing a Si(001) surface to C₆H₅SH produces approximately 3 times as much surface hydrogen as observed in the case of C₆H₅SD exposure.

The FTIR spectrum of liquid benzenethiol is presented in Figure 4c. Liquid benzenethiol has an absorption feature at 2567 cm⁻¹ that has been assigned previously to the sulfur–hydrogen stretching mode.⁴⁷ Absorption features are also found at 3018, 3022, 3050, 3063, and 3073 cm⁻¹ and agree well with the frequencies of the aromatic C–H stretching modes of benzenethiol, as seen in Table 1.⁴⁷ There are no absorption features in the Si–H stretching region between 2000 and 2100 cm⁻¹, nor is there any peak intensity in the region between 2800 and 3000 cm⁻¹. A comparison of the spectra in Figure 4a,c reveals that bonding of benzenethiol to the surface results in a loss of the 2567 cm⁻¹ mode (previously assigned to the sulfur–hydrogen vibration). A new peak, in the region associated with silicon–hydrogen stretching modes, is present at 2086 cm⁻¹.

To investigate the thermal stability and possible decomposition products of the adsorbates, FTIR spectra were obtained after a C₆H₅SD/Si(001) sample was annealed. Figure 5a shows the spectrum of a Si(001) surface initially exposed to 3 L of benzenethiol-SD at 300 K. The silicon sample then was heated to 520 K for 120 s and allowed to cool to 300 K before a second spectrum (Figure 5b) was obtained. This sequential annealing was repeated at 560 K (Figure 5c) and 620 K (Figure 5d). Figure 5e is the spectrum of liquid benzenethiol.

As the temperature is increased to 520 K and greater, the FTIR spectra of C₆H₅SD/Si(001) become simpler and the absorption features become sharper. The high-frequency peaks at 3050 and 3064 cm⁻¹ continue to dominate the spectra, and the relative intensities of these peaks resemble those of the liquid benzenethiol spectrum in Figure 5e. At higher temperatures, as in Figure 5c,d, a small peak at 3100 cm⁻¹ becomes apparent. Two subtle changes also can be noted in the region between

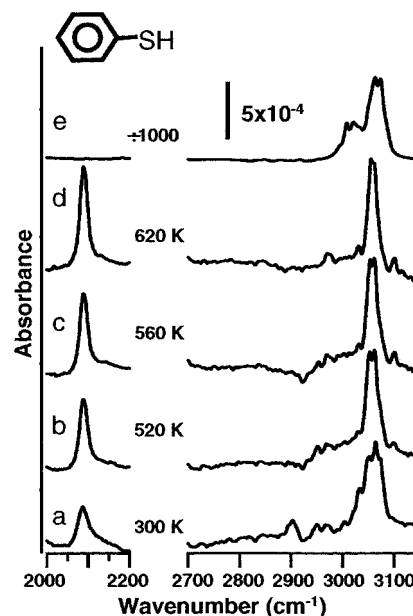


Figure 5. FTIR spectra of benzenethiol-SD: (a) a clean Si(001) surface exposed to 3.0 L (1.0×10^{-8} Torr for 300 s) of benzenethiol-SD at 300 K. Spectra acquired at 300 K after the sample was heated to (b) 520 K, (c) 560 K, and (d) 620 K. (e) For comparison, the FTIR spectrum of liquid benzenethiol also is shown.

2800 and 3000 cm⁻¹. First, the peak at 2908 cm⁻¹ in Figure 5a decreases in intensity as the temperature is increased above 520 K (Figure 5b). Second, the signal in the region between 2940 and 3000 cm⁻¹ increases, resulting in a broad absorption feature. Additionally, the peak intensity at 2087 cm⁻¹ increases as the temperature of the sample is elevated. Comparing the area under the silicon–hydrogen peak at 2087 cm⁻¹ with the area under the silicon–hydrogen peak of a fully saturated monohydride surface, we estimate the peak areas in Figure 5a–d correspond to 0.08, 0.15, 0.27, and 0.31 monolayer, respectively, where one monolayer is equal to 6.8×10^{14} atoms/cm².

Diphenyl Disulfide. Parts a and b of Figure 6 are STM images of a Si(001) surface exposed to 0.24 L of diphenyl disulfide, obtained at a sample bias of -2.20 V. The adsorbed molecules appear as bright protrusions located symmetrically within a single row. All features appear identical, suggesting there is predominantly one surface product. Analysis of images containing step edges allows unambiguous correction for piezo drift and creep. Although we were not able to resolve the individual dimers, this drift correction allows us to estimate that the bright features occupy the space of approximately one dimer but are spaced approximately every other dimer, or 7.7 Å between features. Even at this coverage, the adsorbed molecules emulate the template of the Si(001) dimers and pack into ordered rows. Figure 6c is a schematic drawing indicating the observed positions of the protrusions with respect to the dimers. Height profile measurements indicate the features protrude from the top of the dimers, on average, 0.6 Å.

Figure 7a shows the XPS S(2s) spectrum of a Si(001) surface exposed to 3.0 L of diphenyl disulfide. Fitting these data to a single peak yielded a binding energy of 227.2 eV with a fwhm of 0.99 eV ($\chi^2 = 1.0$). The 227.2 eV binding energy is similar in position to that of benzenethiol adsorbed on Si(001), while the narrow width and the small χ^2 suggest that the majority of sulfur atoms are in a single chemical environment. The C(1s) spectrum for diphenyl disulfide adsorbed on a Si(001) surface (Figure 7b) yielded a single peak with a binding energy of 284.7 eV (fwhm = 1.07 eV, $\chi^2 = 1.0$).

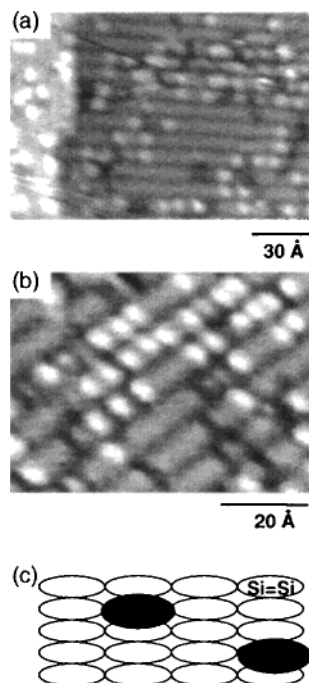


Figure 6. (a, b) STM images of a clean Si(001) surface exposed to 0.24 L (5.0×10^{-10} Torr for 480 s) of diphenyl disulfide at 300 K. The image was acquired at a sample voltage of -2.20 V. Surface adsorbates appear as bright protrusions. (c) Schematic diagram showing the positions of surface adsorbates relative to the silicon dimers. Solid black ovals represent surface adsorbates, while empty ovals represent the silicon dimers.

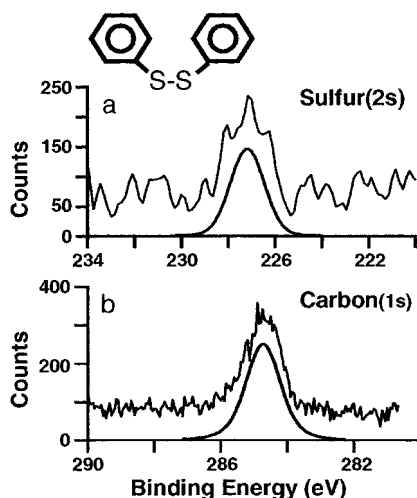


Figure 7. XPS spectra for a clean Si(001) surface exposed to 3.0 L (1.0×10^{-8} Torr for 300 s) of diphenyl disulfide for the (a) S(2s) and (b) C(1s) regions. Solid lines below the data represent fitted peaks.

FTIR spectra of diphenyl disulfide adsorbed on a Si(001) surface are presented in Figure 8. Figure 8a shows the FTIR spectrum of a Si(001) surface exposed to 1.0 L of diphenyl disulfide at 300 K. The dominant features of this spectrum include an unresolved, broad absorption between 3030 and 3048 cm^{-1} and a larger peak at 3063 cm^{-1} . Less prominent is the low-intensity absorption feature at 2077 cm^{-1} , in the silicon-hydrogen stretching region. No changes in the spectrum were observed at higher exposures of diphenyl disulfide; this absence of change indicates that a 1.0 L exposure results in a fully saturated, self-terminating layer.

Figure 8b shows the spectrum of a Si(001) surface exposed to 12.0 L of diphenyl disulfide at a temperature sufficiently low (110 K) to build a multilayer film. This spectrum is nearly

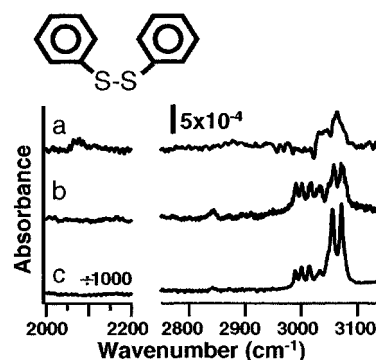


Figure 8. FTIR spectra of (a) a clean Si(001) surface at 300 K exposed to 1.0 L (1.0×10^{-8} Torr for 100 s) of diphenyl disulfide, (b) a clean Si(001) surface at 120 K exposed to 12.0 L (2.0×10^{-8} Torr for 600 s) of diphenyl disulfide, and (c) solid diphenyl disulfide.

identical to the FTIR spectrum of the solid, shown in Figure 8c. The FTIR spectra of a multilayer film and a bulk solid both show six prominent peaks at 2989, 3000, 3014, 3033, 3056, and 3071 cm^{-1} . The lower frequency bands at 2989 and 3000 cm^{-1} are likely combination bands associated with an intact diphenyl disulfide species, while the higher frequency absorptions are similar (± 4 cm^{-1}) to those attributed to C-H stretching modes of the aromatic rings.^{47,48} The similarity of the diphenyl disulfide/Si(001) spectrum acquired at low temperature and the spectrum of the solid suggests that Figure 8b represents the characteristic spectrum of a physisorbed multilayer of diphenyl disulfide on the Si(001) surface.

Discussion

To determine the bonding product(s) of the chemisorption of sulfur-substituted aromatic hydrocarbons on the Si(001) surface, it is necessary to identify (1) whether the ring chemisorbs on the surface, resulting in a loss of π -conjugation, (2) whether the C-S bond, and, in the case of diphenyl disulfide, the S-S bond, remains intact, and (3) whether the source of the surface hydrogen, as evidenced by a strong frequency associated with silicon-hydrogen stretching modes, is primarily due to sulfur-hydrogen or carbon-hydrogen bond cleavage.

Benzenethiol. Preservation of Aromaticity. Direct bonding of the phenyl ring to the Si(001) surface would necessarily result in the formation of new covalent Si-C bonds. Formation of covalent bonds generally occurs most readily through the highest occupied and lowest unoccupied molecular orbitals (HOMO-LUMO) of the reactants. In the case of a phenyl group these HOMO and LUMO orbitals are associated with the π -system of the aromatic ring.⁴ Therefore, if bonding occurs through the phenyl ring, the aromaticity of the molecule is expected to be compromised upon chemisorption, as demonstrated previously for benzene, toluene, and xylene.^{17,18,20-22,24}

The FTIR spectrum of benzenethiol adsorbed on a Si(001) surface (Figure 4a) has strong absorption features above 3000 cm^{-1} . These high-frequency peaks are similar, in both peak position and peak shape, to those arising from aromatic C-H stretching modes of intact benzenethiol, as noted in Table 1. Thus, the IR data suggest that the aromatic ring is unperturbed by adsorption to the surface.

XPS data of benzenethiol also support our conclusion that the aromaticity of the benzenethiol rings remains intact. The small width (1.04 eV fwhm) of the single C(1s) benzenethiol peak at 284.8 eV indicates that there is primarily one species on the surface. Since carbon and sulfur have very similar electronegativities (Pauling electronegativity 2.55 for carbon and 2.58 for sulfur),³⁶ carbon atoms bonded to sulfur atoms are

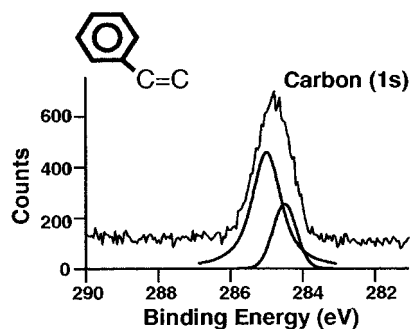


Figure 9. XPS C(1s) spectrum of a clean Si(001) surface exposed to 10 L (5×10^{-8} Torr for 200 s) of styrene at 300 K. The XPS data for styrene yield two C(1s) peaks at 284.5 eV (fwhm = 0.95 eV) and 285.0 eV (fwhm = 0.74 eV) with a reduced χ^2 of 1.0. The peak area ratio of the 284.5 eV peak to the 285.0 eV peak is 1:3. The styrene peak at 284.5 eV is assigned to the two carbon atoms bonded directly to the silicon dimer. We assign the C(1s) peak at 285.0 eV to the six remaining carbons of the intact aromatic ring.

expected to have core-level shifts similar to those of carbon atoms bonded to other carbon atoms. However, since silicon has a much smaller electronegativity (1.90), carbon atoms bonded to silicon are expected to have slightly lower binding energies. For example, previous studies of cyclopentene adsorbed on silicon showed that the carbon atoms bonded directly to the silicon surface yielded a binding energy of 284.0 eV, while the remaining carbon atoms had a binding energy of 284.8 eV.⁴⁹ The 284.8 eV energy observed for benzenethiol is similar to the value of 285.0 eV observed for the intact aromatic ring of styrene (Figure 9) and is clearly distinguishable from the much lower value of ~ 284.0 – 284.5 eV expected for carbon atoms bonded directly to silicon.⁴⁹

Although the majority of the benzenethiol molecules bond to the surface in such a way that the aromaticity of the phenyl ring is retained, our FTIR spectra do show some weak absorbances at 2908 and 2952 cm^{-1} . These frequencies are similar to those of benzene bonded to the Si(001) surface (2899 and 2950 cm^{-1}),²⁴ suggesting that they also arise from direct bonding of the phenyl ring to the surface. We also found that the 2908 and 2952 cm^{-1} peaks disappeared when the sample was briefly heated to 520 K, while the higher intensity peaks associated with intact aromatic species remained present at elevated temperatures. The results of these heating experiments imply that the species adsorbed to the surface through the phenyl ring may be weakly bound or may undergo fragmentation at elevated temperatures. The intact aromatic rings, however, appear thermally stable to temperatures above 520 K. Overall, the FTIR data indicate that the vast majority of species are bonded in such a way that the aromatic ring remains intact. However, a small minority may be weakly adsorbed in a configuration involving bonding of the ring to the surface.

The combination of FTIR and XPS data show several other important features of the chemistry of benzenethiol on Si(001). First, we note that while liquid benzenethiol (Figure 4c) shows a strong S–H vibrational mode at 2567 cm^{-1} , this vibrational mode is absent after the molecule is bonded to the surface (Figure 4a), demonstrating that the sulfur–hydrogen bond is cleaved upon adsorption. Evidence for direct sulfur–silicon bond formation can be obtained from a comparison of sulfur core-level shifts. Other studies have shown that dimethyl sulfide ($\text{CH}_3\text{--S--CH}_3$) bonds to Si(001) via cleavage of one S–C bond, producing adsorbed Si–S–CH₃ species, with an S(2s) binding energy of 227.1 eV.⁵⁰ The 227.3 eV binding energy we observe for benzenethiol is similar, consistent with a similar chemical environment for sulfur in both cases.

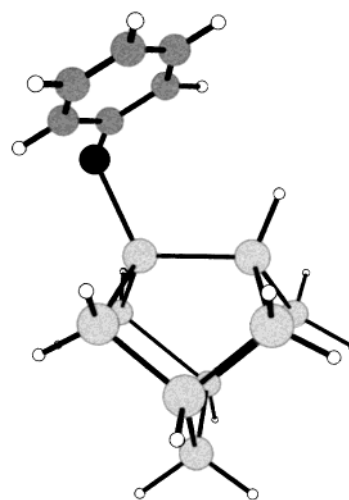


Figure 10. Proposed bonding structure for benzenethiol adsorbed to the surface through a sulfur atom tether. The positions of the atoms represent the calculated lowest energy configuration of this structure. Silicon atoms are light gray, sulfur atoms are black, carbon atoms are dark gray, and hydrogen atoms are white.

At this time, we cannot completely dismiss the possibility that the carbon–sulfur bond of benzenethiol is cleaved upon chemisorption. However, studies in organosilane chemistry and studies of thiol species on gold have shown that the deprotonation of the thiol group is highly favored over carbon–sulfur bond cleavage.^{31,51} Furthermore, predominantly one type of adsorption feature is present in the STM images of benzenethiol on Si(001), slightly off-center with respect to the dimer rows. Feature A, comprising approximately 95% of the bright features in the STM images, is attributed to the S–C₆H₅ species tethered directly to a silicon dimer within a single row.

We propose that the S–H bond of benzenethiol is broken and the resulting S–C₆H₅ fragment bonds to the silicon surface, tethering the aromatic ring to the surface through the sulfur atom. Although the molecular fragment can pivot on the Si–S–C bond, Figure 10 shows the position of the lowest energy configuration for this structure calculated with a Gaussian 98 program utilizing a 6-31+G* basis set, the Becke3LYP density functional, and a nine-atom silicon cluster. Feature A in Figure 2 is assigned to the configuration presented in Figure 10. Feature B in Figure 2 is assigned to carbon fragments or small contaminants on the surface.

S–H vs C–H Bond Cleavage. Cleavage of S–H and/or C–H bonds can be detected in FTIR through the appearance of Si–H vibrations. Because the hydrogen atoms cleaved from adsorbed molecules cannot readily leave the surface as H₂, they remain bound to the underlying silicon surface. Although dehydrogenation of the thiol group would account for the large Si–H peak in Figure 4a, this spectrum alone cannot rule out C–H bond cleavage.

The extent of sulfur–hydrogen versus carbon–hydrogen bond cleavage can be ascertained from isotopic labeling studies comparing C₆H₅SH and C₆H₅SD. NMR spectra of our deuterated benzenethiol show that 92% of the thiol species in our C₆H₅SD sample are deuterated. If only S–D/S–H bond cleavage occurred, we would expect the silicon–hydrogen absorption feature in the FTIR spectrum of the C₆H₅SD/Si(001) to decrease to 8% of the benzenethiol/Si(001) value, from 0.0268 to 0.0021. After the C–H peak area of the C₆H₅SH and C₆H₅SD spectra was normalized to account for changes in alignment between different samples, the silicon–hydrogen peak area of C₆H₅SD/Si(001) in Figure 4b was calculated as 0.0087. This

value is approximately 4 times higher than the area that would be expected if surface hydrogen arose only from sulfur–hydrogen bond cleavage of unlabeled benzenethiol. On the basis of the 92% isotopic purity of our liquid C_6H_5SD , this would suggest that the remaining 0.0066 (or 24% of the total silicon–hydrogen peak area in Figure 4a) is a result of C–H bond cleavage. However, we believe that there may be some isotopic exchange occurring in the vacuum line and/or on the walls of the vacuum chamber, suggesting that the actual contribution to the silicon–hydrogen peak due to C–H bond cleavage is significantly lower. We conclude that the majority of the molecules do not undergo C–H bond cleavage and instead bond via cleavage of the sulfur–hydrogen bond, producing aromatic rings that are nearly unperturbed and tethered to the surface via a Si–S–C linkage.

Diphenyl Disulfide. Preservation of Aromaticity. Both FTIR and XPS data are useful in determining whether the aromatic rings of diphenyl disulfide adsorb on the surface with a loss of aromaticity, like benzene, or remain intact, like styrene and benzenethiol. The FTIR spectrum in Figure 8a of chemisorbed diphenyl disulfide shows only high-frequency peaks. Both the peak shape and the frequencies in Figure 8a bear a strong resemblance to those of the C–H stretching modes of the intact aromatic ring of benzenethiol (Figure 4), indicating that, like benzenethiol, the majority of the rings remain intact as the molecule is chemisorbed. Furthermore, comparison of the XPS data reveals that the carbon(1s) signal at 284.7 eV for diphenyl disulfide adsorbed on the Si(001) surface is similar to the C(1s) binding energy of benzenethiol/Si(001) at 284.8 eV, consistent with the FTIR data showing the aromatic ring is not bonded to the silicon surface. Unlike benzenethiol, diphenyl disulfide has few or no absorption features in the region between 2800 and 3000 cm^{-1} . The absence of peaks in this region suggests that the ring has almost no direct interaction with the surface.

S–S Bond. Studies with disulfide functional groups on gold surfaces have shown that the S–S bond is often broken upon chemisorption.^{27,29,31,52} A sulfur atom (Pauling electronegativity 2.58) is more electronegative than a silicon atom (Pauling electronegativity 1.90).³⁶ Therefore, it is expected that a sulfur atom bonded to a silicon atom would have a slightly higher electron density and would have a small shift to a lower core-level binding energy than an intact S–S species. Indeed, the single peak in the S(2s) region for diphenyl disulfide at 227.2 eV (Figure 7a) is similar in energy to both the S(2s) peak of benzenethiol/Si(001) and the S(2s) peak of dimethyl sulfide/Si(001),⁵⁰ indicating that the sulfur atoms of diphenyl disulfide are covalently bonded to the silicon surface.

From the XPS and FTIR data we conclude that the S–S bond of diphenyl disulfide is cleaved and the two SC_6H_5 fragments are adsorbed to the Si(001) surface through a sulfur tether. Low-coverage STM experiments showed no evidence for asymmetric-looking features, in which two benzenethiol-like SC_6H_5 fragments might be bonded to different dimers. The symmetric nature of the diphenyl disulfide feature lends strong evidence to the idea that the two SC_6H_5 fragments of diphenyl disulfide are adsorbed on a single silicon dimer. We therefore assign the bright features in Figure 6 to the two SC_6H_5 fragments bonded to a single silicon dimer. At higher coverages, the bright features in STM images are aligned with respect to the underlying silicon dimer rows, forming ordered rows of sulfur-tethered aromatic rings.

To better understand the relative positions of the phenyl rings with respect to one another, we performed *ab initio* calculations of our proposed structure of diphenyl disulfide adsorbed on the

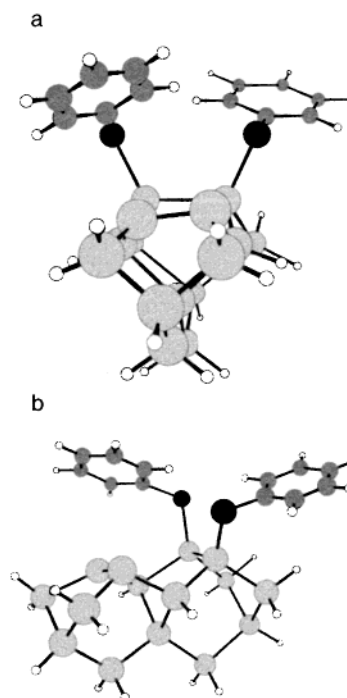


Figure 11. (a) Front and (b) side views of the proposed structure of diphenyl disulfide adsorbed to the surface through the sulfur atom. The positions of the atoms represent the calculated lowest energy configuration of this structure. Silicon atoms are light gray, sulfur atoms are black, carbon atoms are dark gray, and hydrogen atoms are white.

Si(001) surface. Details of this calculation are described elsewhere.²⁵ Briefly, these calculations utilized the Gaussian 98 program,⁵³ using the 6-31+G* basis set, the Becke3LYP density functional, and a 15-atom silicon cluster. Figure 11a,b shows the front and side views, respectively, of the $Si_{15}H_{16}$ cluster that was used to simulate the Si(001) surface and the lowest energy configuration of our proposed structure of diphenyl disulfide bonded to the surface. The lowest energy configuration for this structure shows the aromatic rings twisted away from each other, minimizing the interaction between the π -systems of the phenyl rings.

Bonding Mechanisms. Comparison of the bonding of benzenethiol and diphenyl disulfide with previously studied molecules, namely, phenyl isothiocyanate, or PITC ($C_6H_5-N=C=S$), and styrene, can provide useful insight into the bonding behavior of sulfur-, nitrogen-, and carbon-containing substituent groups and their interaction with the Si(001) surface. The results presented here for benzenethiol and diphenyl disulfide reinforce previous studies of styrene, PITC, and aniline.^{25,54,55} In each case, bonding to the surface occurs with high selectivity through the external substituent group. One unifying factor that may be responsible for this behavior is that the sulfur atoms, nitrogen atoms, and C=C groups in these molecules are all electron-rich and can all act as nucleophiles. This nucleophilic character was shown to be responsible for the ability of simple alkenes, such as cyclopentene, to bond to the Si(001) surface in a facile manner.⁵⁶ The demonstrated selectivity in substituted aromatic systems was identified through *ab initio* calculations exploring the interaction of styrene with the Si(001) surface.²⁵ These calculations showed that there was little or no thermodynamic preference for bonding through the ring versus bonding through the substituent group. Instead, calculations showed that the most important factor in controlling the selectivity of styrene adsorption was the long-range interaction between the molecule and the substrate.²⁵ It was found that the interaction between the vinyl (C=C) group and the surface is attractive if the vinyl group

approaches the surface at the edge of the dimer. In contrast, the interaction between the aromatic ring and the surface dimers was negligible or mildly repulsive.

Overall, the interaction of these substituted aromatic compounds can be thought of as a nucleophilic addition reaction that is strongly facilitated by the ability of the dimers to tilt. This tilting permits transfer of electron density from the "down" atom to the "up" atom of the dimer and enhances the ability of the down atom to act as an electron acceptor for an impinging nucleophile.^{25,56,57} We believe that, likewise, the reason that benzenethiol and diphenyl disulfide bind selectively through the sulfur atoms is that the strong electron-donating character of the sulfur lone pairs facilitates a strong interaction with the Si=Si dimers.

In addition to helping to guide the selectivity of the overall reaction, the electron-rich characteristics of the sulfur group could have significant impact on the electrical properties of the adsorbed S-C₆H₅ fragment. It is worthwhile noting that the apparent heights of the protrusions of both benzenethiol and diphenyl disulfide in the STM images are significantly lower than the expected geometric height of a S-C₆H₅ fragment adsorbed on the Si(001) surface. Benzenethiol has an apparent height of only 0.7(±0.1) Å, almost one-third lower than its expected geometric height of 1.9–2.3 Å. Likewise, the bright features in the STM images corresponding to the S-C₆H₅ fragments of diphenyl disulfide protrude only 0.6(±0.1) Å from the Si(001) surface. Interestingly, the aromatic rings of styrene, tethered to the surface through a carbon atom, appear much taller than the tethered aromatic rings of benzenethiol and phenyl disulfide: styrene has an apparent height of 2.0 Å, close to its geometric height of 2.5 Å.

This significant discrepancy between apparent height and geometric height for sulfur-tethered aromatic rings, especially when compared with carbon-tethered aromatic rings, suggests that the nature of the chemical tether may have significant effects on the STM tunneling properties. This, in turn, implies that the identity of the chemical linkage between the surface and the aromatic ring could significantly influence the electrical transport characteristics through the adsorbed molecule. The results of these preliminary STM studies of benzenethiol and diphenyl disulfide show promise for modifying the electrical properties of adsorbed molecules through careful selection of tethers.

Conclusion

Our results show that thiol and disulfide groups, widely used in the formation of self-assembled monolayers on gold, can be used to selectively attach molecules with aromatic rings to the Si(001) surface. Both benzenethiol and diphenyl disulfide bond to the Si(001) surface via the sulfur atom, leaving the majority of aromatic rings intact and tethered to the surface through a group VI atom. Moreover, the nature of the chemical link may play an important role in controlling the chemical and physical properties of the chemisorbed organic molecules. Ideally, investigations of different chemical functional groups will yield new methods for selectively attaching molecules to surfaces via a variety of different chemical and structural tethers.

Acknowledgment. This work was supported in part by a grant from the National Science Foundation (CHE-007138).

References and Notes

- (1) Yates, J. T., Jr. *Science* **1998**, 279, 335.
- (2) Aviram, A.; Ratner, M. A. *Chem. Phys. Lett.* **1974**, 29, 277.
- (3) Mirkin, C. A.; Ratner, M. A. *Annu. Rev. Phys. Chem.* **1992**, 43, 719.
- (4) Brédas, J. L.; Cornil, J.; Beljonne, D.; dos Santos, D. A.; Shuai, Z. *Acc. Chem. Res.* **1999**, 32, 267.
- (5) Tour, J. M.; Jones, L., II; Pearson, D. L.; Lamba, J. J. S.; Burgin, T.; Whitesides, G. M.; Allara, D. L.; Parikh, A. N.; Atre, S. V. *J. Am. Chem. Soc.* **1995**, 117, 9529.
- (6) Bumm, L. A.; Arnold, J. J.; Cygan, M. T.; Dunbar, T. D.; Burgin, T. P.; Jones, L., II; Allara, D. L.; Tour, J. M.; Weiss, P. S. *Science* **1996**, 271, 1705.
- (7) Andres, R. P.; Bielefeld, J. D.; Henderson, J. I.; Janes, D. B.; Kolagunta, V. R.; Kubiak, C. P.; Mahoney, W. J.; Osifchin, R. G. *Science* **1996**, 273, 1690.
- (8) Cygan, M. T.; Dunbar, T. D.; Arnold, J. J.; Bumm, L. A.; Shedlock, N. F.; Burgin, T. P.; Jones, L., II; Allara, D. L.; Tour, J. M.; Weiss, P. S. *J. Am. Chem. Soc.* **1998**, 120, 2721.
- (9) Ishida, T.; Mizutani, W.; Akiba, U.; Umemura, K.; Inoue, A.; Choi, N.; Fujihira, M.; Tokumoto, H. *J. Phys. Chem. B* **1999**, 103, 1686.
- (10) Reed, M. A.; Zhou, C.; Muller, C. J.; Burgin, T. P.; Tour, J. M. *Science* **1997**, 278, 252.
- (11) Muller, C. J.; Vleeming, B. J.; Reed, M. A.; Lamba, J. J. S.; Hara, R.; Jones, L., II; Tour, J. M. *Nanotechnology* **1996**, 7, 409.
- (12) Ventra, M. D.; Pantelides, S. T.; Lang, N. D. *Appl. Phys. Lett.* **2000**, 76, 3448.
- (13) Arkin, M. R.; Stemp, E. D. A.; Holmlin, R. E.; Barton, J. K.; Hormann, A.; Olson, E. J. C.; Barbara, P. F. *Science* **1996**, 273, 475.
- (14) Murphy, C. J.; Arkin, M. R.; Jenkins, Y.; Ghatia, N. D.; Bossmann, S. H.; Turro, N. J.; Barton, J. K. *Science* **1993**, 262, 1025.
- (15) Aich, P.; Labuik, S. L.; Tari, L.; Delbaere, L. J. T.; Roesler, W. J.; Falk, K. J.; Steer, R. P.; Lee, J. S. *J. Mol. Biol.* **1999**, 294, 477.
- (16) Wallace, P. R. *Phys. Rev.* **1947**, 71, 622.
- (17) Taguchi, Y.; Fujisawa, M.; Takaoka, T.; Okada, T.; Nishijima, M. *J. Chem. Phys.* **1991**, 95, 6870.
- (18) Jeong, H. D.; Ryu, S.; Lee, Y. S.; Kim, S. *Surf. Sci. Lett.* **1995**, 344, L1226.
- (19) Borovsky, B.; Krueger, M.; Ganz, E. *Phys. Rev. B* **1998**, 57, R4269.
- (20) Kong, M. J.; Teplyakov, A. V.; Lyubovitsky, J. G.; Bent, S. F. *Surf. Sci.* **1998**, 411, 286.
- (21) Lopinski, G. P.; Moffatt, D. J.; Wolkow, R. A. *Chem. Phys. Lett.* **1998**, 282, 305.
- (22) Lopinski, G. P.; Fortier, T. M.; Moffatt, D. J.; Wolkow, R. A. *J. Vac. Sci. Technol., A* **1998**, 16, 1037.
- (23) Wolkow, R. A.; Lopinski, G. P.; Moffatt, D. J. *Surf. Sci.* **1998**, 416, L1107.
- (24) Coulter, S. K.; Hovis, J. S.; Ellison, M. D.; Hamers, R. J. *J. Vac. Sci. Technol., A, Part 2* **2000**, 18, 1965–1970.
- (25) Schwartz, M. P.; Ellison, M. D.; Coulter, S. K.; Hovis, J. S.; Hamers, R. J. *J. Am. Chem. Soc.* **2000**, 122, 8529.
- (26) Bandyopadhyay, K.; Patil, V.; Sastry, M.; Vijayamohan, K. *Langmuir* **1998**, 14, 3808.
- (27) Szafranski, C. A.; Tanner, W.; Laibinis, P. E.; Garrell, R. L. *Langmuir* **1998**, 14, 3570.
- (28) Whelan, C. M.; Barnes, C. J.; Walker, C. G. H.; Brown, N. M. D. *Surf. Sci.* **1999**, 425, 195.
- (29) Nuzzo, R. G.; Fusco, R. A.; Allara, D. L. *J. Am. Chem. Soc.* **1987**, 109, 2358.
- (30) Prime, K. L.; Whitesides, G. M. *Science* **1991**, 252, 1164.
- (31) Jung, C.; Dannenberger, O.; Xu, Y.; Buck, M.; Grunze, M. *Langmuir* **1998**, 14, 1103.
- (32) Porter, M. D.; Bright, T. B.; Allara, D. L.; Chidsey, C. E. D. *J. Am. Chem. Soc.* **1987**, 109, 3559.
- (33) Bain, C. D.; Whitesides, G. M. *J. Am. Chem. Soc.* **1988**, 110, 3665.
- (34) Dishner, M. H.; Hemminger, J. C.; Feher, F. J. *Langmuir* **1996**, 12, 6176.
- (35) Dishner, M. H.; Feher, F. J.; Hemminger, J. C. *Chem. Commun.* **1996**, 16, 1971.
- (36) Pauling, L. *The Nature of the Chemical Bond*, 3rd ed.; Cornell University: Ithaca, NY, 1960.
- (37) Appelbaum, J. A.; Baraff, G. A.; Hamann, D. R. *Phys. Rev. B* **1976**, 14, 588.
- (38) Hamers, R. J.; Tromp, R. M.; Demuth, J. E. *Phys. Rev. B* **1986**, 34, 5343.
- (39) Chabal, Y. J. *Surf. Sci. Rep.* **1988**, 8, 211.
- (40) Shan, J.; Wang, Y.; Hamers, R. J. *J. Phys. Chem.* **1996**, 100, 4961.
- (41) Hamers, R. J.; Tromp, R. M.; Demuth, J. E. *Surf. Sci.* **1987**, 181, 246.
- (42) Shirley, D. A. *Phys. Rev. B* **1972**, 5, 4709.
- (43) Bevington, P. R. *Data Reduction and Error Analysis for the Physical Sciences*; McGraw-Hill Book Co.: New York, 1992.
- (44) Abbott, D. J.; Colonna, S.; Stirling, S. J. M. *J. Chem. Soc., Perkin Trans. 1* **1976**, 492.
- (45) Tanner, D. D.; Samal, P. W.; Ruo, T. C.-S.; Henriquez, R. J. *Am. Chem. Soc.* **1979**, 101, 1168.
- (46) Shen, W.; Nyberg, G. L.; Liesegang, J. *Surf. Sci.* **1993**, 298, 143.

- (47) Varsanyi, G. *Assignments for Vibrational Spectra of Seven Hundred Benzene Derivatives*; Akademiai Kiado and J. Wiley & Sons: Budapest, 1974; p 94.
- (48) Green, J. H. S. *Spectrochim. Acta* **1968**, 24A, 1624.
- (49) Liu, H.; Hamers, R. J. *Surf. Sci.* **1998**, 416, 354–362.
- (50) Liu, J.; Hamers, R. J. Manuscript in preparation.
- (51) Becker, B.; Wojnowski, W. *Synth. React. Inorg. Met.-Org. Chem.* **1984**, 14, 537.
- (52) Bandyopadhyay, K.; Vijayamohan, K.; Venkataraman, M.; Pradeep, T. *Langmuir* **1999**, 15, 5314.
- (53) Frisch, M. J.; Trucks, G. W.; Sclegel, H. B.; Scuseria, G. E.; Robb, M. A.; Cheeseman, J. R.; Zakrzewski, V. G.; Montgomery, J. A., Jr.; Stratmann, R. E.; Burant, J. C.; Dapprich, S.; Millam, J. M.; Daniels, A. D.; Kudin, K. N.; Strain, M. C.; Farkas, O.; Tomasi, J.; Barone, V.; Cossi, M.; Cammi, R.; Mennucci, B.; Pomelli, C.; Adamo, C.; Clifford, S.; Ochterski, J.; Petersson, G. A.; Ayala, P. Y.; Fui, Q. C.; Morokuma, K.; Malick, D. K.; Raback, A. D.; Raghavachari, K.; Foresman, J. B.; Cioslowski, J.; Ortiz, J. V.; Baboul, A. G.; Stefanov, B. B.; Liu, G.; Liashenko, A.; Piskorz, P.; Komaromi, I.; Gomperts, R.; Martin, R. L.; Fox, D. J.; Keith, T.; Al-Laham, M. A.; Peng, C. Y.; Nanayakkara, A.; Gonzalez, C.; Challacombe, M.; Gill, P. M. W.; Johnson, B.; Chen, W.; Wong, M. W.; Andres, J. L.; Gonzalez, C.; Head-Gordon, M.; Replogle, E. S.; Pople, J. A. *Gaussian 98*, Revision A.7; Gaussian Inc.: Pittsburgh, 1998.
- (54) Ellison, M. D.; Hamers, R. J. *J. Phys. Chem. B* **1999**, 103, 6243.
- (55) Cao, X.; Coulter, S. K.; Ellison, M. D.; Liu, H.; Liu, J.; Hamers, R. J. *J. Phys. Chem. B*, in press.
- (56) Hamers, R. J.; Coulter, S. K.; Ellison, M. D.; Hovis, J. S.; Padowitz, D. F.; Schwartz, M. P. *Acc. Chem. Res.* **2000**, 33, 617.
- (57) Choi, C. H.; Gordon, M. S. *J. Am. Chem. Soc.* **1999**, 121, 11311.